

HELIOSEISMOLOGICAL TEST OF A NEW MODEL FOR STELLAR CONVECTION

L. PATERNÒ

Istituto di Astronomia dell'Università di Catania, Città Universitaria, Viale A. Doria 6, 95125 Catania, Italy

R. VENTURA

Osservatorio Astrofisico di Catania, Città Universitaria, Viale A. Doria 6, 95125 Catania, Italy

V. M. CANUTO

NASA, Goddard Institute for Space Studies, 2880 Broadway, New York, NY 10025

AND

I. MAZZITELLI

Istituto di Astrofisica Spaziale CNR, CP 67, 00044 Frascati, Italy

Received 1992 January 13; accepted 1992 July 13

ABSTRACT

We compare the predictions of two solar models with the observed p -mode eigenfrequencies. The two models use the same input microphysics (nuclear reaction rates, opacity, and equation of state) and the same numerical evolutionary code, *but differ in the treatment of turbulent convection*. The first model employs the standard mixing-length theory of convection (MLT), while the second model employs a new model of turbulent convection (CM) whose primary goal was that of accounting for the whole spectrum of turbulent eddies so as to avoid the MLT approximation that such a wide spectrum be represented by a single, large eddy. With the suggestion that the mixing length, Λ , be taken to be z , the distance to the nearest convective boundary, the new CM model has no free parameters, and yet it predicts a solar T_{eff} to within 0.5%. The $\Lambda = z$ suggestion, within the context of the MLT, would yield T_{eff} of by $\simeq 3\%$ that forces the introduction of $\Lambda = \alpha H_p$, with α a free, adjustable parameter.

The main result of this paper is that the p -mode eigenfrequencies calculated with the CM model show an overall improvement with respect to those calculated with the standard MLT model.

Subject headings: convection — Sun: interior — Sun: oscillations — turbulence

1. INTRODUCTION

For many years the lack of a viable alternative to the mixing-length theory of convection (MLT) has forced astrophysicists who model stellar structure and evolution of work with a model which has the practical advantages of being easy to implement but which is based on a set of drastic approximations more appropriate for a moderately viscous fluid than for the almost inviscid stellar interiors.

Although numerical simulations of turbulent convection have recently become available (Chan & Sofia 1986; Stein & Nordlung 1989; Hossain & Mullan 1990), their inclusion in stellar evolutionary codes would result in a prohibitive demand of computer time.

More recently, a new approach to the problem of stellar turbulent convection has been proposed by Canuto & Mazzitelli (1991, 1992; henceforth cited as CM1, CM2), the CM model, which overcomes some of the drastic approximations of the mixing length theory.

In particular, the more correct treatment of some basic features of low Prandtl number turbulent convection vis à vis the MLT treatment has improved the predictive power of the model which can easily be employed in evolutionary codes (CM1).

In order to further test to what extent the CM model has improved the description of turbulent convection vis à vis the standard MLT model, we calculate the p -mode eigenfrequencies as predicted by the two models and compare them with the helioseismological data obtained at the Big Bear Solar Observatory during 1986–1987 by Libbrecht, Woodard, & Kaufman (1990). The data set is an upgraded version of the

data published by Duvall et al. (1988) and Libbrecht & Kaufman (1988) and was kindly supplied to us by F. Hill.

2. MODELS AND CODES

2.1. Convection Theory

The mixing length theory, which originated with the pioneering work of G. I. Taylor and L. Prandtl, was first applied to the stellar case by L. Biermann. The version currently used in most evolutionary codes is due to Böhm-Vitense (1958).

In this theory, a fluid element rises under the effect of buoyancy, travels with a characteristic velocity through a mean free path, or mixing length, then breaks up and merges with the surroundings. Velocity components of the consequent smaller scale motions and associated temperature fluctuations are assumed to be uncorrelated, so there is no contribution from them to the overall heat transport (Gough 1977).

The mixing length model treats turbulence as quasi-incompressible (c_v is substituted for c_p and the temperature gradient ∇ is measured with respect to its adiabatic counterpart ∇_{ad}). A considerably more severe approximation is the treatment of the wide spectrum of turbulent eddies as if it were dominated by a single large eddy with size comparable to the local pressure scale height. While this may be a reasonable approximation for viscous fluids, which are indeed characterized by a rather narrow eddy spectrum, it fails when applied to the nearly inviscid stellar interiors, where the ratio of the largest to the smallest eddy may be $\simeq 10^8$.

The CM approach, while retaining quasi-incompressibility, accounts for the full spectrum of turbulent eddies using the direct interaction approximation (DIA; Leslie 1973) and the

(eddy damped quasi-normal Markovian (EDQNM; Lesieur 1989) models to treat the nonlinear interactions. The model derives a new expression for the turbulent convective flux and for the turbulent pressure, the latter usually ignored in the MLT. At high convective efficiencies, the new turbulent flux is up to 10 times larger than the MLT flux, whereas at low efficiencies, the new flux is lower than the MLT flux. This indicates that the new flux has an altogether different relationship toward convective efficiency than the MLT model. We may also note that a larger convective flux is in agreement with the work of Chan & Sofia (1989) as well as with the recent numerical simulation of turbulent convection by Cabot et al. (1990), who found that the MLT free parameter had to be scaled up to a factor of 7–8 in order to match the numerical results.

Since the standard MLT does not provide an expression for the mixing length, Λ , it is usually suggested that Λ be taken as $\Lambda = \alpha H_p$, where H_p is the local pressure scale height; the free parameter α is then adjusted to reproduce the observed position of a given star in the H-R diagram. The procedure usually yields values of α larger than unity, in contrast with some of the basic assumptions of the mixing length treatment.

The CM model sets $\Lambda = z$, where z is the distance between the point at which the superadiabatic gradient is computed and the top of the convection zone. The value of z at each point is found as the result of an eigenvalue problem, thus freeing the model of the presence of a free parameter. We may note that the same relation $\Lambda = z$ would yield poor results within the MLT (CM1, CM2).

As recently shown in CM2, the model yields a solar T_{eff} within 0.5% of the observed value. In that sense, the application of the CM model to evolutionary studies can be said to be free of adjustable parameters.

Recently, two of the authors have proposed a refined version of the $\Lambda = z$ model so as to account for local effects. As discussed in CM2, to the extent one is interested in evolutionary studies only, the new refinement is quite unnecessary since the results clearly demonstrate that the nonlocal nature embodied in the $\Lambda = z$ relation does indeed capture the bulk of the mixing length.

The new, more general expression for Λ is $\Lambda = \alpha(S)z$, where $\alpha(S)$ is a calculable function of S (the latter is related to the convective efficiency by eqs. [7] and [8] of CM1). The function α does, however, also depend on a new variable, called a in CM2, such that $1 - a$ represents the contribution of local effects to the mixing length. The expression of $\alpha(S, a)$ is given in equation (9) of CM2. By tuning the value of a , one can achieve a fit to the solar T_{eff} even better than 0.5%, but this is not the spirit nor the reason only it was introduced, a point that we shall take up again in § 2.2 below.

2.2. Evolutionary Code

The evolutionary code used to produce the MLT and CM models of the present Sun is described in detail elsewhere (Mazzitelli 1989 and references therein). It is basically a standard code for stellar evolution and may not differ significantly from codes of other authors.

The numerical integration follows the Newton-Raphson scheme, with the local mass as independent variable along all the structure, including the superadiabatic subsurface regions. The fit to the optical atmosphere is at $\tau = \frac{2}{3}$.

A fine zoning has been adopted for the internal structure, mainly in the convective region, the total number of mesh

points ranging from 900 to 1100 along the evolutionary path. More than half of the mesh points are always in the region from the surface to the base of the convection zone.

The chemical evolution scheme makes use of the linearization procedure by Arnett & Truran (1969) and a simple zero order Runge-Kutta integration for the initial convective core. Each of the physical time steps required by the model to reach the present age, starting from a chemically homogeneous Sun, is subdivided in 10 smaller steps, along which the chemical evolution is computed, allowing also for convective mixing when and where required. Since ~ 100 physical time steps are required before the small initial convective core disappears (complete CNO and ${}^3\text{He}$ relaxation), and 200 further physical time steps are necessary for the model to reach the present solar luminosity, the total number of chemical evolution time steps is ~ 3000 .

The radiative opacities adopted for low temperatures ($T < 6000$ K) are those computed by Kurucz (1992) and for higher temperatures are those by Iglesias & Rogers (1991), both based on the Anders-Grevesse mixture (Anders & Grevesse 1989). It is worth noticing that, in the range of temperatures $6000 \text{ K} \leq T \leq 10,000 \text{ K}$, both opacities give similar results. The values of the opacity at a given temperature, density, and chemical composition are obtained by quadratic interpolations of the tabulated values.

The equation of state and the related thermodynamic quantities are those computed by Magni & Mazzitelli (1979).

The nuclear network accounts for the complete p - p chain, including beryllium branch, and CNO cycle, without forcing the elements to equilibrium. The cross sections are taken from Harris et al. (1983), and the weak and intermediate screening effects from Graboske, De Witt, & Grossman (1973).

Both MLT and CM models reach the present luminosity of the Sun ($L_{\odot} = 3.846 \times 10^{33} \text{ ergs s}^{-1}$) after 4.7 billion years of evolution with initial values $Z = 0.018$ and $Y = 0.285$.

Since in helioseismological studies the value of the solar radius is crucial, within the MLT we had to tune carefully the value of α so as to obtain the value of the present solar radius ($R_{\odot} = 6.9599 \times 10^{10} \text{ cm}$) at $L = L_{\odot}$ within four significant figures. This procedure leads to a value $\alpha = 1.7473$ with the convection zone base ($\nabla - \nabla_{\text{ad}} = 0$) located at $r_b = 0.735 R_{\odot}$.

As already discussed in § 2.1, the CM model does not require, in principle, any tuning, since the solar radius is correctly obtained as the result of the computations. Specifically, with $\Lambda = z$, the value of the predicted solar radius differs by less than 1% from R_{\odot} (less than 0.5% in T_{eff} ; CM2, Fig. 2). This small difference, altogether immaterial in stellar evolution studies, becomes extremely important for the present comparison.

The more refined version of the original CM1 model (CM2) takes into account, besides the dominant nonlocal effects represented by $\Lambda = \Lambda(z) = z$, also the local contribution to the mixing length, $\Lambda = \Lambda(l, z)$, where l represents local variables. The latter effect may be especially important at the top and bottom of the convection zone. The improved CM2 model thus includes a parameter, a , which represents the relative strength of the nonlocal versus the local effects, with $a = 1$ corresponding to $\Lambda = z$. The sensitivity of the solar radius to the variation of the parameter a is very weak, but sufficient to tune its value within the fourth decimal figure in order to obtain exactly R_{\odot} . With the present model we obtained $a = 1.91$ to fit exactly R_{\odot} at L_{\odot} . Even though a is an adjust-

able parameter, *its role cannot be compared with that of the MLT α parameter*, since the latter can dramatically effect the value of solar radius, whereas a cannot. Therefore, the CM model can still be considered a model which does not require a free parameter to fit the present solar radius and T_{eff} . Stated differently, while the MLT model contains the first-order free parameter, α , the CM2 model contains only the second-order adjustable parameter, a . The results of the CM2 computations give $\nabla = \nabla_{\text{ad}}$ at $r_b = 0.735 R_{\odot}$, as in the MLT case. This is not surprising, since the depth of the convection zone is controlled by the total luminosity.

Both the MLT and CM models yield, of course, the same effective temperature ($T_{\text{eff}} = 5785$ K).

The two models are therefore comparable in that they have the same L_{\odot} and R_{\odot} , use the same input microphysics (equation of state, nuclear reaction rates, and opacities) and the same numerical code. The difference lies in the treatment of convective transport. Differences in the predicted p -mode eigenfrequencies should therefore be ascribed to the different treatment of convection.

We fitted the surface of the models ($\tau = \frac{2}{3}$) to the HSRA atmosphere model (Gingerich et al. 1971) to reach the temperature of 4170 K ($\tau \cong 10^{-4}$) at the minimum.

2.3. Oscillation Codes

In order to compute the radial and nonradial p -mode adiabatic eigenfrequencies we use two numerical codes. The first has been developed by Dziembowski (1971) and makes use of the complete set of the four first-order ordinary differential equations, which include the perturbation of the gravitational potential. This code has been used to compute eigenfrequencies up to $l = 100$. For $l > 100$, we use a second, faster code developed by Gough and Paternò (Belvedere, Gough, & Paternò 1983), which makes use of the Cowling approximation.

Both codes use the same outer boundary conditions taken at $T = 4170$ K, namely, the solutions match onto a causal linear eigenfunction of the plane-parallel isothermal atmosphere. The causal eigenfunctions are those which correspond to forcing from below, excluding the possibility of incoming waves from infinity or evanescent motions produced by pressure perturbations from above.

The first code uses the standard inner boundary conditions usually taken near the center. The second code is used only for modes with $l > 100$. Since these modes have the turning point well above the center, in order to speed up the calculations, we start the integration at some level below the turning point, with the boundary condition of vanishing radial perturbation at that level.

We carried out some numerical tests to verify the accuracy of the eigenfrequency calculations for the two CM and MLT models.

The first test was based on the construction of models with an increasing number of radial mesh points, until a frequency convergence to a limit model was found. This limit model had 3079 mesh points, but yet a model with 2075 mesh points gave frequency differences of about a hundredth of a microhertz with respect to the limit model. The models used in this paper have ~ 1000 mesh points (CM, 1032; MLT, 993), and their error is below $1 \mu\text{Hz}$ for a large variety of modes with $5 \leq n \leq 33$ and $0 \leq l \leq 100$. This test can be compared with an analogous one carried out by Guenther & Serajedini (1988) for the mode $l = 1$, $n = 17$, reported in their Figure 1. In that

figure a difference of about $+2 \mu\text{Hz}$ can be seen between 1000 and 3000 mesh point models. This difference is sensibly larger than our difference of $+0.49 \mu\text{Hz}$ for the same mode. The reason for that probably depends on the way the equilibrium models for oscillation codes are constructed. We calculated accurately the derivative quantities which are used in the oscillation codes. Derivatives were obtained analytically by a third-order polynomial fitting to the mesh-points of the models. The result was a smoother behavior of all the quantities with the consequence of increasing the numerical accuracy without requiring a very large number of mesh points.

The second test was to verify to what extent the eigenfunctions of the high radial order modes ($n = 33$) were spatially resolved with our 1000 mesh point models. A comparison between the eigenfunctions of the 1000 mesh-point models with those of the 3079 mesh-point limit model showed that the nodes were completely resolved and the eigenfunctions overlapped with a high degree of accuracy, the only visible effect being a frequency difference smaller than $1 \mu\text{Hz}$.

The third test was concerned with the use of the Cowling approximation for the $l > 100$ modes, with the inner boundary condition of vanishing radial perturbation taken at some level below the mode turning points. The comparison between the eigenfrequencies calculated with non-Cowling and Cowling approximation codes showed that the frequency differences decrease rapidly with increasing l and, although less rapidly, with decreasing n . Since we start to use the Cowling approximation code by $l = 200$, and high l -modes contain only low radial orders, the error of our calculations, using the Gough & Paternò's code, is smaller than $0.01 \mu\text{Hz}$ for all the calculated modes. The comparison between the Gough & Paternò's code, with the inner boundary condition of vanishing radial perturbation taken at some level below the mode turning points, and the Dziembowski's code (used in the Cowling approximation option), with standard inner boundary conditions taken at the center, showed no differences in either the eigenfrequencies or the eigenfunctions.

In conclusion, numerical errors in eigenfrequencies determined by our oscillation calculations are smaller than $1 \mu\text{Hz}$ for all the considered modes, and thus any difference larger than $1 \mu\text{Hz}$ should be attributed to the physics and assumptions of the model, when comparing models with observations, and to the different treatment of convection, when mutually comparing models.

3. MODEL COMPARISON SCHEME

In view of a helioseismological p -mode analysis and as the waves propagate with the sound speed $c_s = [\Gamma_1 p / \rho]^{1/2}$, this seems to be the most appropriate quantity to highlight the structural differences of the two models. The differences in the p -mode eigenfrequencies should in fact reflect the differences in c_s between the models. In this context, we also look at the well-known helioseismological variable:

$$v_0 = \left(2 \int_0^{R_{\odot}} \frac{dr}{c_s} \right)^{-1}; \quad (1)$$

the quantity (1), which is the inverse of twice the sound travel time from the surface of the Sun to its center, is most sensitive to the structure of the layers very close to the Sun's surface (Provost 1984), where the major differences between the models are expected to occur.

In the asymptotic analysis (Tassoul 1980), valid for $n \gg l$, the quantity (1) is closely related to the first-order frequency separation between modes with the same l 's, and with n 's differing by one unity, namely, $\Delta\nu_0 = \nu_{n,l} - \nu_{n-1,l}$.

A second comparison is based on the analysis of modes with $0 \leq l \leq 11$, following the procedure described in Dziembowski, Paternò, & Ventura (1988). This analysis allows us to gain information on the regions responsible for the deviations of the theoretical eigenfrequencies either from those of another model or from the observed ones.

Variations in frequency $\delta\nu$, associated with small changes in the structure of the equilibrium model, depend on the frequency ν and the harmonic degree l of the modes. They can be expressed as (Dziembowski, Paternò, & Ventura 1988):

$$\delta\nu(\nu, l) = \frac{\int_0^{R_\odot} (\delta\mathcal{L}\xi) \cdot \xi^* d^3x}{E(\nu, l)}, \quad (2)$$

where $\delta\mathcal{L}$ is a linear operator which depends on the modifications of the model structure, ξ is the eigenfunction, and $E(\nu, l)$ is the mode energy defined in Christensen-Dalsgaard (1986).

The energy of modes with $l < 20$ does not depend on l , but only on ν (Christensen-Dalsgaard 1986). Consider a surface layer whose thickness is $r_e \leq r \leq R_\odot$, and choose $r_e \gg r_c = c_s[l(l+1)]^{1/2}/2\pi\nu$, namely, well above the mode turning point r_c . In this layer, the motions are nearly vertical and the mode eigenfunctions do not depend on l , but only on ν . This allows us to split the integral in the expression (2) into two parts: the first depends on l and ν in the region $r < r_e$, while the second depends only on ν in the region $r > r_e$. In so doing, the source of inaccuracies in the models can be identified by looking at the behavior of $\delta\nu$ as a function of frequency for modes with $0 \leq l \leq 11$.

The shallowest turning point for these modes is the one related to the mode with the highest degree ($l = 11$) and the lowest frequency ($\nu = 1320 \mu\text{Hz}$; radial order $n = 5$), namely, $r_c = 0.55 R_\odot$. Thus we can safely take $r_e = r_b = 0.735 R_\odot$, which is the base of the convection zone in both the MLT and CM models.

The region above r_e can be further separated into two regions: an inner region in which the asymptotic approximation ($\nu \gg |dc_s/dr|/2\pi$) holds and an outer region close to the surface. The separation boundary, determined by the above condition, can be set at $r_i = 0.95 R_\odot$, where $|dc_s/dr|/2\pi \cong 210 \mu\text{Hz}$, a value considerably lower than the lowest frequency of the modes considered here.

If the frequency differences were originating from sound speed differences in the region $r_e \leq r \leq r_i$, where asymptotics applies, the same straight line dependence on ν should attain for all l 's (Dziembowski, Paternò, & Ventura 1988). Therefore, we are able to distinguish three regions responsible for differences in the mode frequencies: (1) a first region, $0 \leq r \leq r_e$, in which $\delta\nu = f(\nu, l)$; (2) a second region, $r_e \leq r \leq r_i$, in which $\delta\nu = a\nu + b$ with a and b constants; (3) a third region, $r_i \leq r \leq R_\odot$, in which $\delta\nu = g(\nu)$.

A third comparison concerns the behavior of the frequency differences between models and observations for some modes with l ranging from 40 to 1300, so as to verify which of the eigenfrequencies of the two models is closer to the observed values. With increasing l and decreasing frequency, or n , the mode propagation region is shifted toward the surface and becomes thinner. This again allows us to estimate where the most important deviations from an ideal solar model arise.

4. RESULTS AND DISCUSSION

As apparent from Figure 1, the relative difference between the sound speed of the MLT and CM models is negligible throughout the Sun, except in the outmost layers ($0.95 R_\odot \leq r \leq R_\odot$), where it is of the order of a few percent. This is hardly surprising since the most noticeable difference between the two treatments of turbulent convection occurs in the superadiabatic layers.

To this regard, we would like to mention some very recent results by Dziembowski, Pamyatnykh, & Sienkiewicz (1992). The authors, using a variational method, were able to find the corrections to the quantities $p/\rho = c_s^2/\Gamma_1$ and ρ to be applied to a solar standard model so as to reproduce the observed p -mode frequencies. They used the same opacities and element mixture as those used by us, and a MLT model. Their results show that, in the outmost layers, the quantity p/ρ should be 2% less than that of the standard MLT model. This variation is consistent with the CM sound speed trend, and implies that the variation in sound speed should be of the order of 4% if Γ_1 does not vary. Similarly they found that, in a very thin layer close to the surface, the density should be some 10% lower than that of the standard MLT model, again in agreement with the CM model (CM1, Fig. 11).

In the layers above $0.65 R_\odot$ the CM sound speed is lower than that of the MLT: thus, the CM eigenmodes should have smaller frequencies than those of the MLT model, especially the high l modes trapped in the superadiabatic layers. This fact is related to the high convective efficiency of CM with respect to MLT, which produces a shallower temperature gradient in the superadiabatic layers as reflected in the lower sound speed.

We computed $\Delta\nu_0$ as the average frequency separation between modes with $l = 0$ with n 's ranging from 12 to 33, i.e.,

$$\Delta\nu_0 \equiv \overline{\Delta\nu_0} = \sum_{n=13}^{33} (\nu_{n,0} - \nu_{n-1,0})/21;$$

for a proper comparison, the range of the radial orders considered has been chosen on the basis of the available observational data. The results yield $\Delta\nu_0(\text{MLT}) = 136.92 \mu\text{Hz}$, with standard deviation $\sigma(\text{MLT}) = 1.67 \mu\text{Hz}$ and range of variation

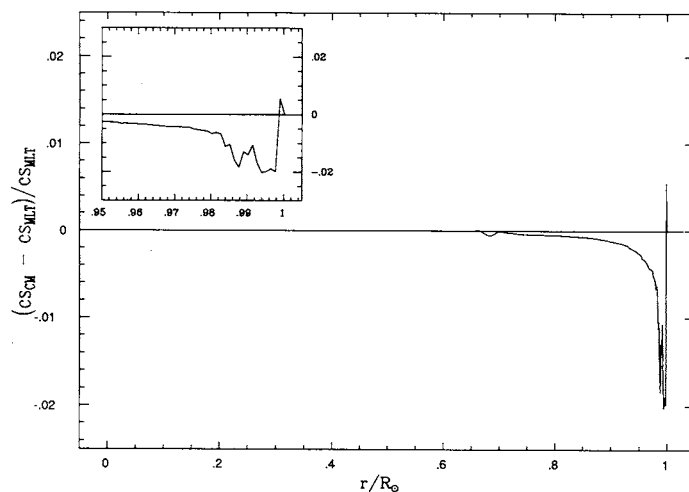


FIG. 1.—Relative sound speed difference between the CM and MLT models, $(CS_{\text{CM}} - CS_{\text{MLT}})/CS_{\text{MLT}}$, as a function of the Sun's fractional radius. The small frame shows the behavior of the same quantity in an enlarged portion of the surface layers.

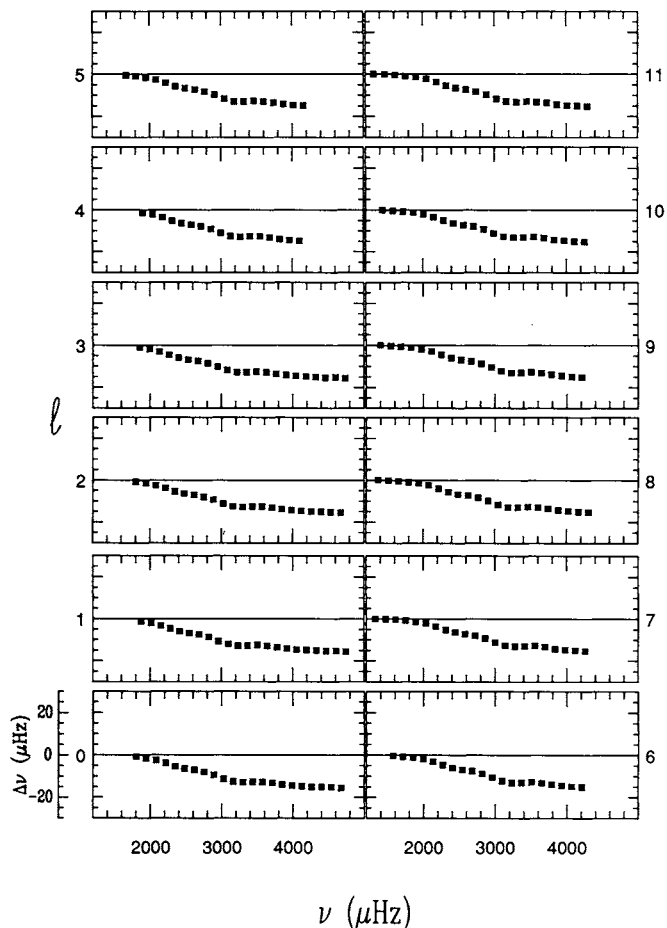


FIG. 2.—Frequency differences between CM and MLT models, $\Delta\nu(\mu\text{Hz}) = \nu_{\text{CM}} - \nu_{\text{MLT}}$, as functions of the MLT model frequencies for modes with $0 \leq l \leq 11$.

$r(\text{MLT}) = 6.24 \mu\text{Hz}$, and $\Delta\nu_0(\text{CM}) = 136.23 \mu\text{Hz}$, with $\sigma(\text{CM}) = 2.00 \mu\text{Hz}$ and $r(\text{CM}) = 6.76 \mu\text{Hz}$, to be compared with the observational value $\Delta\nu_0(\text{obs}) = 135.49 \mu\text{Hz}$, with $\sigma(\text{obs}) = 1.29 \mu\text{Hz}$ and $r(\text{obs}) = 4.50 \mu\text{Hz}$.

The comparison shows that the CM model yields a mean value closer to the observed value than MLT model, even though the spread and range are slightly larger. As already stated, this depends on the different structural characteristics of the layers near the surface where different treatments of turbulent convection produce the largest effects. This is also evident by comparing our result with that derived from a very recent solar standard model (Guenther et al. 1992; Table 2A) which gives $\Delta\nu_0 = 137.15 \mu\text{Hz}$, with $\sigma = 1.45 \mu\text{Hz}$ and $r = 4.64 \mu\text{Hz}$.

Inspection of Figure 2 reveals that the l -dependence of the frequency differences $\Delta\nu$'s is negligible, since all the curves are parallel. In addition, since the dependences on ν are not straight lines, the differences between the two models arise only from the layers above $r_i = 0.95 R_\odot$, as already mentioned in § 3.

This fact also validates our helioseismological analysis to ascertain which of the two treatments of turbulent convection is more appropriate to describe the Sun, in that it demonstrates that we are comparing two almost identical models which differ only in the region where the effects of a correct treatment of turbulence are more important. Differences in eigen-

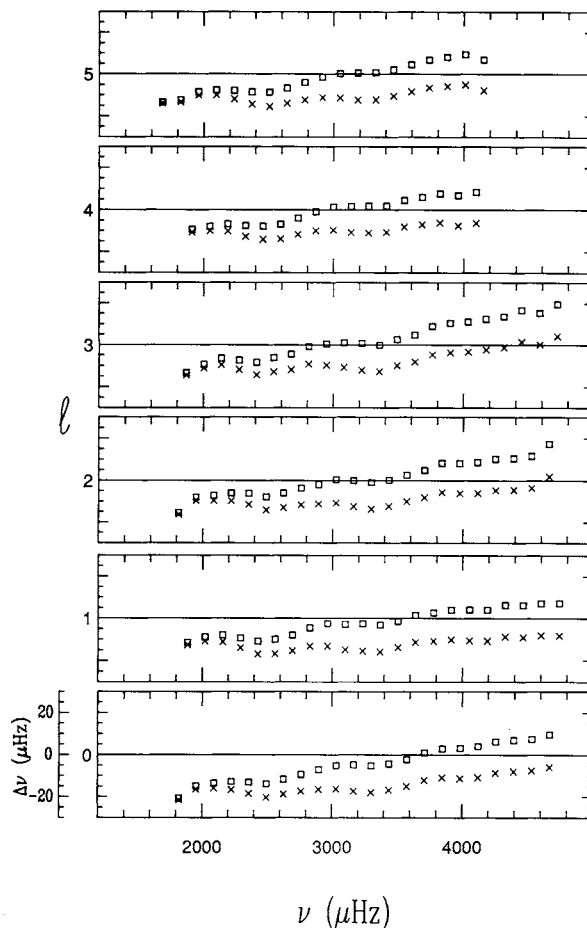


FIG. 3.—Frequency differences between MLT model and observations, $\Delta\nu(\mu\text{Hz}) = \nu_{\text{MLT}} - \nu_{\text{obs}}$ (squares), and CM model and observations, $\Delta\nu(\mu\text{Hz}) = \nu_{\text{CM}} - \nu_{\text{obs}}$ (crosses), as functions of the observed frequencies for modes $0 \leq l \leq 5$.

frequencies of up to $15 \mu\text{Hz}$ can be seen in Figure 2, with $|\Delta\nu|$ increasing with frequency, the eigenfrequencies of the CM model being systematically lower than those of the MLT model.

Figures 3 and 4 highlight the difference of each model with observations. Here, even though the dependence of $\Delta\nu$ on ν is dominant, a slight dependence on l cannot be ruled out. The ν -dependence appears less pronounced in the CM model than in the MLT model, indicating an improvement in the treatment of the surface layers. A least-square linear fit of data indicates, in fact, that the slopes $|\Delta\nu/\nu|$ relative to the CM model are systematically lower than those of the MLT model, ranging from a factor of 2 ($l = 0$) to a factor of 20 ($l = 11$). However, both models indicate that the treatment of the surface layers is still a problem. The small l -dependence may also indicate that the physics of the solar interior needs revisions. The differences between theoretical and observed eigenfrequencies range from -20 to $+20 \mu\text{Hz}$, well above the accuracy of observations, which is of the order of few tenths of microhertz in this range of l 's.

In Figures 5–8 we compare MLT and CM eigenfrequencies with the observed values for some high-degree modes with l ranging from 40 to 1300. For all the values of l we have examined, the CM eigenfrequencies are, in general, closer to observations than the MLT eigenfrequencies. In the range $40 \leq l \leq 200$, deviations of the MLT model range from -20 to

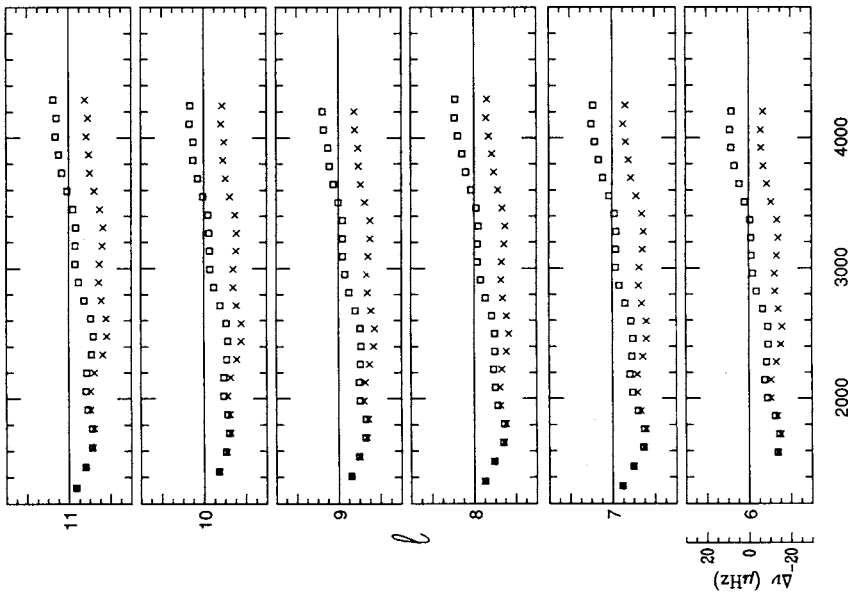


FIG. 4.

FIG. 4.—Frequency differences between MLT model and observations, $\Delta\nu(\mu\text{Hz}) = \nu_{\text{MLT}} - \nu_{\text{obs}}$ (squares), and CM model and observations, $\Delta\nu(\mu\text{Hz}) = \nu_{\text{CM}} - \nu_{\text{obs}}$ (crosses), as functions of the observed frequencies for modes $6 \leq l \leq 11$.

FIG. 5.—Frequency differences between MLT model and observations, $\Delta\nu(\mu\text{Hz}) = \nu_{\text{MLT}} - \nu_{\text{obs}}$ (squares), and CM model and observations, $\Delta\nu(\mu\text{Hz}) = \nu_{\text{CM}} - \nu_{\text{obs}}$ (crosses), as functions of the radial order n for the modes with $l = 40, 60, 80,$ and 100 . The straight line on the top of the figure indicates the turning points of the modes, r_c , in terms of the solar radius. The deepest point refers to the mode with the lowest l and highest n , while the shallowest one refers to the mode with the highest l and the lowest n . Modes with intermediate n 's and l 's have intermediate penetrations.

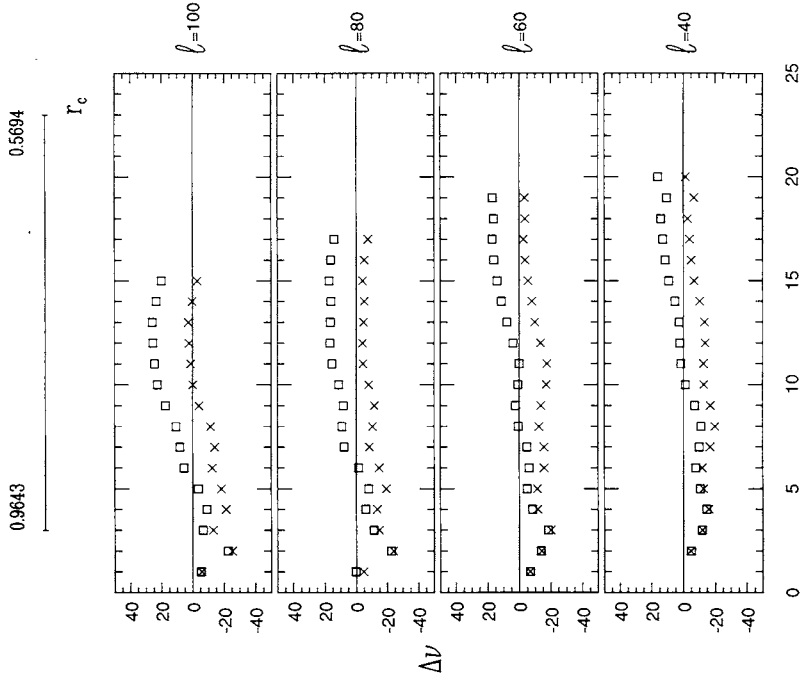


FIG. 5.

FIG. 5.

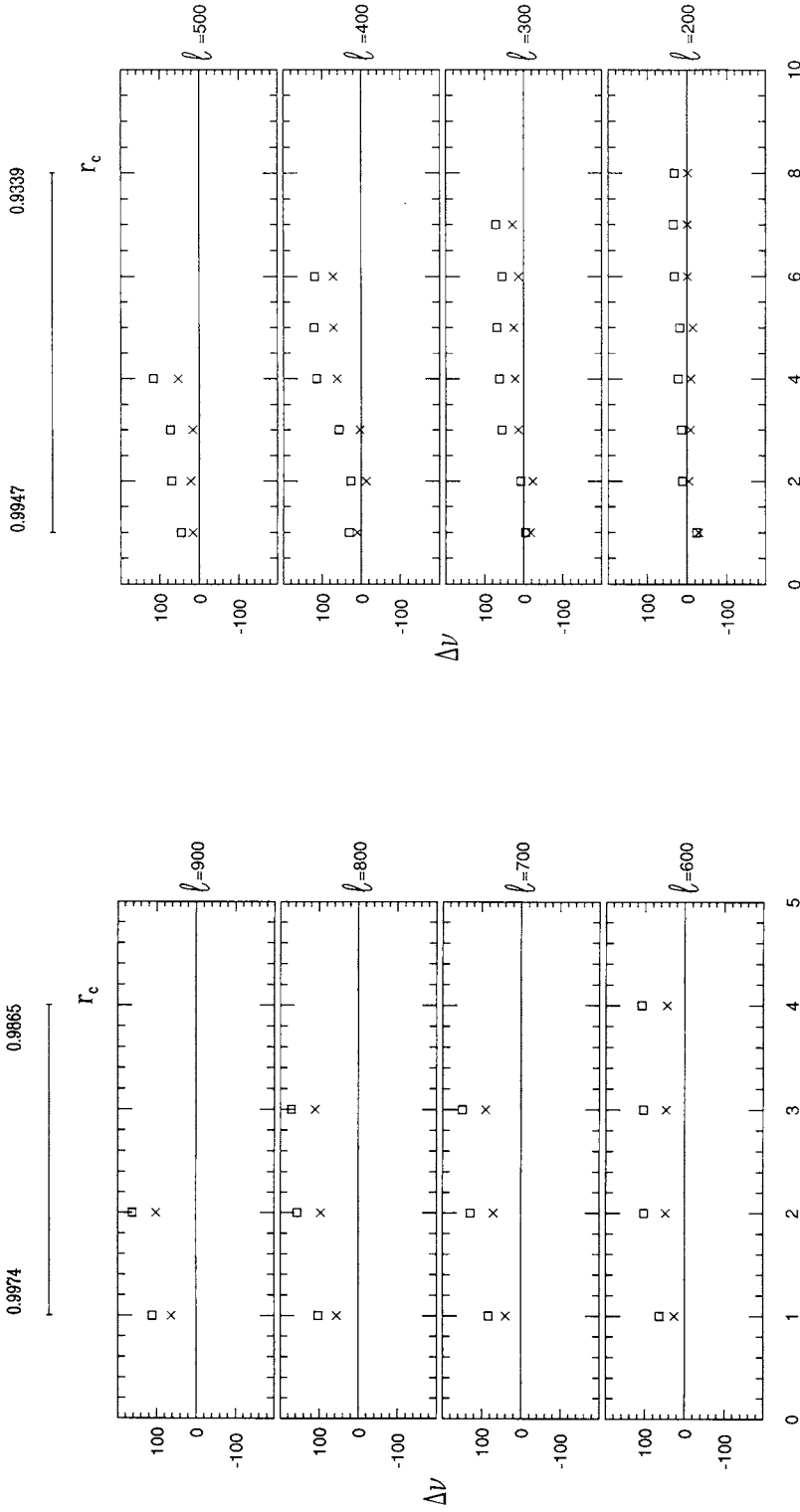


FIG. 6

FIG. 7

FIG. 6.—Frequency differences between MLT model and observations, $\Delta\nu(\mu\text{Hz}) = \nu_{\text{MLT}} - \nu_{\text{obs}}$ (squares), and CM model and observations, $\Delta\nu(\mu\text{Hz}) = \nu_{\text{CM}} - \nu_{\text{obs}}$ (crosses), as functions of the radial order n for the modes with $l = 200, 300, 400,$ and 500 . The straight line on the top of the figure indicates the turning points of the modes, r_c , in terms of the solar radius. The deepest point refers to the mode with the lowest l and highest n , while the shallowest one refers to the mode with the highest l and the lowest n . Modes with intermediate n 's and l 's have intermediate penetrations.

FIG. 7.—Frequency differences between MLT model and observations, $\Delta\nu(\mu\text{Hz}) = \nu_{\text{MLT}} - \nu_{\text{obs}}$ (squares), and CM model and observations, $\Delta\nu(\mu\text{Hz}) = \nu_{\text{CM}} - \nu_{\text{obs}}$ (crosses), as functions of the radial order n for the modes with $l = 600, 700, 800,$ and 900 . The straight line on the top of the figure indicates the turning points of the modes, r_c , in terms of the solar radius. The deepest point refers to the mode with the lowest l and highest n , while the shallowest one refers to the mode with the highest l and the lowest n . Modes with intermediate n 's and l 's have intermediate penetrations.

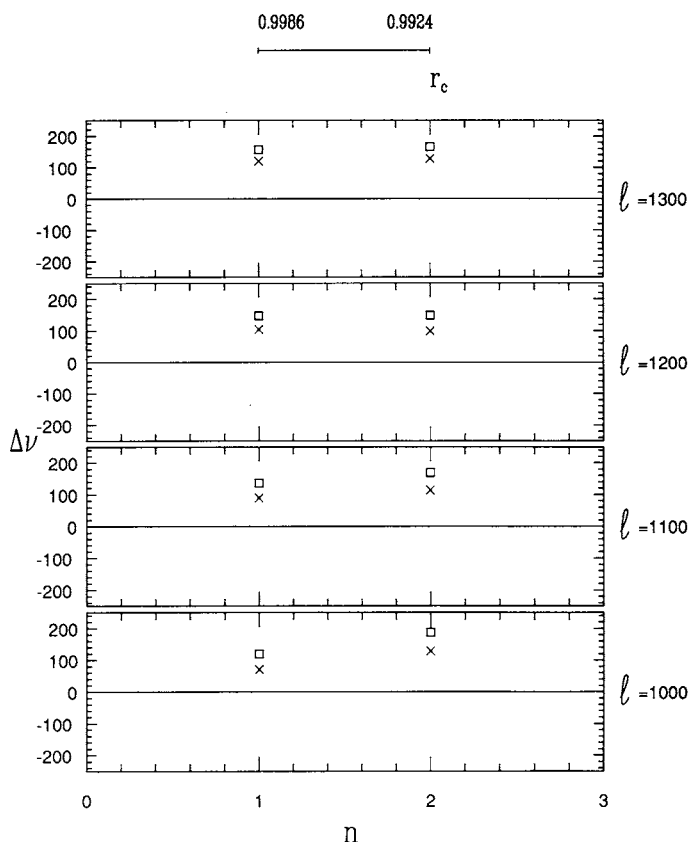


FIG. 8.—Frequency differences between MLT model and observations, $\Delta\nu(\mu\text{Hz}) = \nu_{\text{MLT}} - \nu_{\text{obs}}$ (squares), and CM model and observations, $\Delta\nu(\mu\text{Hz}) = \nu_{\text{CM}} - \nu_{\text{obs}}$ (crosses) as functions of the radial order n for the modes with $l = 1000, 1100, 1200$ and 1300 . The straight line on the top of the figure indicates the turning points of the modes, r_c , in terms of the solar radius. The deepest point refers to the mode with the lowest l and highest n , while the shallowest one refers to the mode with the highest l and the lowest n . Modes with intermediate n 's and l 's have intermediate penetrations.

+40 μHz , while those of the CM model range from -20 to 0 μHz . In the range above $l = 200$, the deviations tend to increase with l , and, in the range above $l = 400$, the deviations are always positive.

This indicates that the theoretical sound speed in the convection zone is overestimated by both the MLT and CM models, although in the CM model the deviations are sensibly smaller.

For modes with $400 \leq l \leq 900$, they range from few microhertz to 100 μHz , while the MLT deviations range from 30 to 180 μHz . The largest deviations occur in the range $1000 \leq l \leq 1300$, which concerns modes trapped in a very thin surface layer ($\approx 0.006 R_{\odot}$). Here, even though the CM deviations are smaller than those of MLT model, there is a tendency to converge to the same value for both the models. This depends on the very sharp increase of the CM sound speed near the surface.

Observational errors for the very high degree modes ($l > 400$) are quite large, of the order of some tens of microhertz. The deviations we are reporting here are nonetheless real and should be attributed to deviations of the models from the real Sun.

5. CONCLUSIONS

In Figs. 1 and 2 we compare the predictions of two solar models with the same microphysics input, but which differ significantly in the treatment of stellar convection in the layers very close to the surface.

Notwithstanding problems in the treatment of the interior (i.e., uncertainties in the opacities, equation of state and nuclear reaction cross sections), the present analysis shows that both MLT and CM models suffer from inadequacies in the treatment of the surface layers. However, since these inadequacies are common to both models, the results should only reflect the different treatments of turbulent convection.

The overall assessment is that the new CM model predicts eigenfrequencies closer to the observed values than the standard MLT. The relevance of this conclusion lies in the fact that the improvement has been achieved without adjustable parameters of the first order, like α in the MLT, but only through the calibration of a second-order parameter, like a in the CM2, to obtain the solar radius within the required accuracy of the fourth decimal figure.

We wish to thank F. Hill for providing us the most recent helioseismological data, W. A. Dziembowski for lending his numerical code and for useful discussions, W. Däppen, P. Demarque, and D. Guenther for useful discussions and suggestions.

L. Paternò and R. Ventura are grateful to the Gruppo Nazionale di Astronomia-CNR for supporting this research under contract CN90.01206.02.

Numerical calculations have been carried out with the CONVEX C210 of the Osservatorio Astrofisico di Catania.

REFERENCES

- Anders, E., & Grevesse, N. 1989, *Geochim. Cosmochim. Acta*, 53, 197
 Arnett, W. D., & Truran, J. W. 1969, *ApJ*, 157, 359
 Belvedere, G., Gough, D. O., & Paternò, L. 1983, *Sol. Phys.*, 82, 343
 Böhm-Vitense, E. 1958, *Z. Astrophys.*, 46, 108
 Cabot, W., Hubickyj, O., Pollak, J. B., Cassen, P., & Canuto, V. M. 1990, *Geophys. Astrophys. Fluid Dyn.*, 53, 1
 Canuto, V. M., & Mazzitelli, I. 1991, *ApJ*, 370, 295 (CM1)
 ———. 1992, *ApJ*, 389, 724 (CM2)
 Chan, K. L., & Sofia, S. 1986, *ApJ*, 307, 222
 ———. 1989, *ApJ*, 336, 1022
 Christensen-Dalsgaard, J. 1986, in *Seismology of the Sun and Distant Stars*, ed. D. O. Gough, (Dordrecht: Reidel), 23
 Duvall, T. L., Harvey, J. W., Libbrecht, K. G., Popp, B. D., & Pomerantz, M. A. 1988, *ApJ*, 324, 1158
 Dziembowski, W. A. 1971, *Acta Astron.*, 21, 289
 Dziembowski, W. A., Pamyatnykh, A. A., & Sienkiewicz, R. 1992, *Acta Astron.*, in press
 Dziembowski, W. A., Paternò, L., & Ventura, R. 1988, *A&A*, 200, 213
 Gingerich, O., Noyes, R. W., Kalkofen, W., & Cuny, Y. 1971, *Sol. Phys.*, 18, 347
 Gough, D. 1977, in *Lecture Notes in Physics, Problems of Stellar Convection*, ed. E. A. Spiegel & J. P. Zahn (Berlin: Springer), 15
 Graboske, H. C., De Witt, H. E., & Grossman, H. S. 1973, *ApJ*, 181, 457
 Guenther, D. B., Demarque, P., Kim, Y. C., & Pinsonneault, M. H. 1992, *ApJ*, 387, 372
 Guenther, D. B., & Serajedini, A. 1988, *ApJ*, 327, 933
 Harris, M. J., Fowler, W. A., Cauglan, G. R., & Zimmerman, B. A. 1983, *ARA&A*, 21, 165
 Hossain, M. H., & Mullan, D. J. 1990, *ApJ*, 354, L33
 Iglesias, C. A., & Rogers, F. J. 1991, *ApJ*, 371, 408
 Kurucz, R. L. 1992, in *NATO ASI Ser., Stellar Atmospheres: Beyond the Classical Models*, ed. L. Crivellari, I. Hubney, & D. G. Hummer (Dordrecht: Kluwer), in press
 Lesieur, M. 1989, *Turbulence in Fluids* (Dordrecht: Nijhoff)
 Leslie, D. C. 1973, *Developments in the Theory of Turbulence* (Oxford: Clarendon)
 Libbrecht, K. G., & Kaufman, J. M. 1988, *ApJ*, 324, 1172
 Libbrecht, K. G., Woodard, M. F., & Kaufman, J. M. 1990, *ApJS*, 74, 1129
 Magni, G., & Mazzitelli, I. 1979, *A&A*, 72, 134
 Mazzitelli, I. 1989, *ApJ*, 340, 249
 Provost, J. 1984, in *Observational Tests of the Stellar Evolution Theory*, ed. A. Maeder & A. Renzini (Dordrecht: Reidel), 47
 Stein, R. F., & Nordlund, Å. 1989, *ApJ*, 342, L95
 Tassoul, M. 1980, *ApJS*, 43, 469